Intracellular Transport, Assembly, and Degradation of Wild-Type and Disease-linked Mutant Gap Junction Proteins

Judy K. VanSlyke,* Suzanne M. Deschenes,[†] and Linda S. Musil*[‡]

*Vollum Institute for Advanced Biomedical Research and [†]Department of Molecular and Medical Genetics, Oregon Health Sciences University, Portland, Oregon 97201

More than 130 different mutations in the gap junction integral plasma membrane protein connexin32 (Cx32) have been linked to the human peripheral neuropathy X-linked Charcot–Marie–Tooth disease (CMTX). How these various mutants are processed by the cell and the mechanism(s) by which they cause CMTX are unknown. To address these issues, we have studied the intracellular transport, assembly, and degradation of three CMTX-linked Cx32 mutants stably expressed in PC12 cells. Each mutant had a distinct fate: E208K Cx32 appeared to be retained in the endoplasmic reticulum (ER), whereas both the E186K and R142W mutants were transported to perinuclear compartments from which they trafficked either to lysosomes (R142W Cx32) or back to the ER (E186K Cx32). Despite these differences, each mutant was soluble in nonionic detergent but unable to assemble into homomeric connexons. Degradation of both mutant and wild-type connexins was rapid ($t_{1/2} < 3$ h) and took place at least in part in the ER by a process sensitive to proteasome inhibitors. The mutants studied are therefore unlikely to cause disease by accumulating in degradation-resistant aggregates but instead are efficiently cleared from the cell by quality control processes that prevent abnormal connexin molecules from traversing the secretory pathway.

INTRODUCTION

Charcot–Marie–Tooth (CMT) 1 disease is the name given to a heterogeneous group of dominant disorders that collectively are the most common form of inheritable disease in the peripheral nervous system (Murakami *et al.*, 1996). The X-linked form of CMT 1 disease (CMTX) is a progressive demyelinating neuropathy characterized clinically by moderately reduced nerve conductance velocities. Manifestations of CMTX typically include weakness and atrophy of the distal limb muscles, sensory loss in feet, lower legs, and hands, pes cavus deformity, and decreased or absent deep tendon reflexes (reviewed by Bone *et al.*, 1997). The severity of symptoms varies considerably between affected families and in males ranges from mild impairment to being wheel-chair-bound by age 50 y (Ionasescu *et al.*, 1996; Deschenes *et al.*, 1997).

In 1993, CMTX was genetically linked to defects in the gene encoding the tetra-spanning integral plasma membrane protein connexin32 (Cx32) (Bergoffen *et al.*, 1993). Cx32, like other members of the connexin protein family, forms gap junctions in vertebrate tissues. Gap junctions are collections of transmembrane channels that serve as low-resistance pathways for the diffusion of substances <1 kDa in molecular mass including ions, metabolites, and second messengers (Goodenough *et al.*, 1996). Usually, gap junctions form between two neighboring cells, creating intercellular conduits that relay messages between, and maintain metabolic continuity within, connected cells. In contrast, uninjured myelinating Schwann cells do not make gap junctions with each other or with neuronal cells. Instead, Cx32 appears to form gap junctions between adjoining wraps of myelin within the sheath of a single Schwann cell at the incisures of Schmidt–Lanterman and the paranodal region. This creates a radial pathway for the diffusion of substances that has been estimated to be up to 1000 times shorter than the circumferential route (Scherer *et al.*, 1995; Balice-Gordon *et al.*, 1998). Although the function of these intracellular gap junctions is unclear, possibilities include dissipation of potassium gradients generated by neuronal activity and trans-

myelin transport of small trophic and signaling molecules. Mice with a targeted deletion of the Cx32 gene, although normal when young, gradually develop a progressive demyelinating neuropathy with histological features similar to those observed in human CMTX patients (Anzini *et al.*, 1997; Scherer *et al.*, 1998).

More than 130 different mutations in Cx32 have been identified in CMTX patients (Bone *et al.*, 1997). Essential to elucidating the molecular mechanisms underlying CMTX and the basis for genotype and phenotype correlations is determining how defects in the Cx32 gene disrupt connexin function. The great majority of CMTX-linked Cx32 mutations result in changes in single amino acid residues that could affect channel formation, activity, and/or metabolic stability. As determined from structural and biochemical analysis, the first step in gap junction formation is the noncovalent oligomerization of six connexin monomers into a hexameric annular structure known as a connexon. After transport to the cell surface, two connexons on apposing plasma membranes dock to form what is usually an intercellular channel, but which in Schwann cells instead links adjacent myelin wraps. Last, these channels pack at up to $10,000/\mu m^2$ into paracrystallin arrays known as gap junctional plaques (reviewed by Musil, 1994). Despite this complex assembly process, there is no evidence that gap junction formation requires any nonconnexin protein(s). Another remarkable aspect of gap junctions is the rapid turnover rate of connexins, which are degraded in a wide variety of cultured and in vivo systems with a $t_{1/2}$ of only 1.5–5 h even after incorporation into gap junctional plaques (Fallon and Goodenough, 1981; Musil *et al.*, 1990; Beardslee *et al.*, 1998).

To date, it has not been possible to maintain either endogenous or exogenous Cx32 protein expression in cultured Schwann cells (Scherer *et al.*, 1995; Yoshimura *et al.*, 1998), necessitating the use of other systems for the in vitro study of CMTX-linked Cx32 mutants. When transfected into otherwise connexin-deficient PC12 cells, several Cx32 point mutants, including R142W, E186K, and E208K, showed no detectable staining on the plasma membrane but instead appeared to be defective in intracellular transport (Deschenes *et al.*, 1997). The R142W Cx32 mutant also accumulated intracellularly when expressed under the control of the myelin-specific P_o promotor in the Schwann cells of either Cx32 knock-out or otherwise normal mice (Bone *et al.*, 1997; Scherer *et al.*, 1999). Both R142W/− and R142W/+ mice showed age-dependent demyelination and remyelination of peripheral nerve. In R142W/+ animals, endogenous Cx32 was no longer detectable in the myelin sheath but instead was localized to the same intracellular compartments as the R142W Cx32 mutant. Dominant-negative activity of intracellularly retained CMTX-linked Cx32 mutants has also been reported by Omori *et al.* (1996) in HeLa cell transfectants. Taken together, these observations illustrate the potential for certain CMTX-linked Cx32 mutants to have gain-of-function effects and indicate that transfected PC12 cells are a suitable system to study mutant trafficking.

Mutations in plasma membrane or secreted proteins that inhibit transport to the cell surface can cause disease by one of two general mechanisms (Kim and Arvan, 1998; Aridor and Balch, 1999). Aridor and Balch (1999) have defined class I mutations as those that prevent transport of the affected protein to the plasma membrane but do not interfere with its ability to be efficiently degraded. Disease results from the absence of the wild-type protein, and any proteins associated with it, from the cell surface. In contrast, class II mutations inhibit the turnover as well as the intracellular transport of the affected protein. Accumulation of undegraded protein can then induce chronic endoplasmic reticulum (ER) stress responses, which in turn may lead to major changes in cell physiology such as apoptosis, abnormal differentiation, and altered proliferation. A class II-type mechanism has been proposed for mutants of proteolipid protein that cause Pelizaeus–Merzbacher disease (Gow and Lazzarini, 1996; Gow *et al.*, 1998) and of peripheral myelin protein 22 that result in CMT type 1A (D'Urso *et al.*, 1998; Aridor and Balch, 1999). By analogy, toxic accumulation of Cx32 (also a tetraspanning integral plasma membrane protein of myelin) has been suggested as a mechanism for some CMTX-linked Cx32 mutants (Deschenes *et al.*, 1997), although this contention has not been experimentally addressed.

One possibility consistent with the phenotypic variation observed in CMTX patients is that different defects in Cx32 lead to distinct transport, assembly, and degradative fates. That differences in intracellular processing can be associated with separate disease mechanisms is illustrated by the finding that mutants of the water channel aquaporin-2 that are restricted to the ER are linked with recessive nephrogenic diabetes insipidus, whereas those that are arrested in the Golgi cause a dominant form of the disease, apparently because of formation of mixed oligomers with wild-type aquaporin-2 (Kamsteeg *et al.*, 1999). Given the aforementioned deleterious effects of intracellular accumulation of undegraded mutant proteins, it is particularly important to delineate the pathways by which mutant and wild-type connexins are turned over. The lysosome has generally been considered the major means of proteolysis of membrane-associated proteins and has been shown to participate in the turnover of gap junctional plaques (Larsen and Tung, 1978). Recent evidence has, however, indicated that the proteasome is involved in the degradation of many membrane-bound and soluble proteins within the secretory pathway (Brodsky and McCracken, 1997). This includes wild-type connexin43 (Cx43), whose turnover rate has been reported to be reduced by proteasomal inhibitors (Laing and Beyer, 1995). The role of the proteasome in the turnover of wild-type (WT) Cx32 is not known, nor has the mechanism of degradation of mutant connexins been addressed.

In the current study, we present the first integrated analysis of the intracellular transport, assembly, and degradation of CMTX-linked Cx32 mutants. We use a combination of biochemical and morphological techniques to examine the post-translational fate of the R142W, E186K, and E208K CMTX-linked Cx32 mutants expressed in stable transfectants of PC12 cells. Our results provide new insights into the pathophysiology of CMTX disease as well as into the quality control mechanisms that govern the fidelity of assembly of connexins into gap junctional plaques.

MATERIALS AND METHODS

Cell Culture

The generation of multiple independent clonal lines of PC12J cells (a subclone of rat pheochromocytoma cells devoid of endogenous gap junction activity) stably expressing either wild-type human Cx32 or

a CMTX-linked Cx32 mutant has been described by Deschenes *et al.* (1997). In brief, the coding regions of wild-type or mutant (E208K, R142W, or E186K) Cx32 were amplified from the genomic DNA of control subjects or CMTX patients, respectively, and subcloned into the pREP9 expression vector for transfection; vector-only transfectants served as controls. Cell lines were maintained in RPMI 1640 medium supplemented with 10% horse serum, 5% FCS, penicillin G, streptomycin, and 400 μg/ml G418 (Deschenes *et al.*, 1997). Expression of endogenous Cx32 in the rat hepatoma cell line MH$_1$C$_1$ (a generous gift from R. Ruch, Medical College of Ohio, Toledo, OH) was enhanced by culturing for 48 h in the presence of 10 μM dexamethasone as previously described (Ren *et al.*, 1994). Mouse sarcoma cells stably transfected with the adhesion molecule liver cell adhesion molecule (L-CAM) (S180L) (Mege *et al.*, 1988) were maintained in Dulbecco's modified Eagle's medium plus 10% FCS, penicillin G, and streptomycin, and Chinese hamster ovary (CHO)-K1 cells were maintained in F-12 medium containing 10% FCS.

Antibodies and Reagents

Mouse monoclonal antibody 7C6.C7 specific for Cx32 was a generous gift of E. Hertzberg (Albert Einstein College of Medicine, Bronx, NY) and used for all immunofluorescence microscopy. For immunoprecipitation of Cx32, crude antiserum from rabbits immunized with a synthetic peptide corresponding to amino acids 98–124 of rat Cx32 (kindly provided by D. Goodenough, Harvard Medical School, Boston, MA; Goodenough *et al.*, 1988) was used in pulse–chase experiments, whereas affinity-purified polyclonal rabbit anti-Cx32 immunoglobulin G (IgG) purchased from Zymed (San Francisco, CA; 71-0600) was used for cross-linking analysis. Cx43 was immunoprecipitated with affinity-purified polyclonal rabbit anti-Cx43 antibodies prepared as previously described (Musil *et al.*, 1990), and L-CAM was immunoprecipitated with a polyclonal rabbit antiserum kindly provided by W. Gallin (University of Alberta, Edmonton, Alberta, Canada). Marker proteins for the ER (calreticulin) and Golgi stack (mannosidase II) were immunodetected using monospecific polyclonal rabbit antisera from Affinity BioReagents (Golden, CO; PA3-900) and K. Moreman (University of Georgia, Athens, GA), respectively. FITC-conjugated donkey anti-mouse IgG (Jackson ImmunoResearch, West Grove, PA) and rhodamine-conjugated goat anti-rabbit IgG (Pierce, Rockford, IL) were used as secondary antibodies.

Unless otherwise noted, all reagents were from Sigma (St. Louis, MO). Stock solutions of proteasomal inhibitors were prepared in DMSO at the following concentrations and stored at $-20°C$: 26 mM *N*-acetyl-leu-leu-norleucinal (ALLN), 1 mM lactacystin, and 5 mM carboxybenzyl-leucyl-leucyl-leucyl-vinylsulphone (ZL$_3$VS). ZL$_3$VS was a kind gift from M. Bogyo (Harvard Medical School). A concentrated stock of chloroquine (10 mM) was freshly prepared in double-distilled H$_2$O (ddH$_2$O) for each experiment. Other reagents were stored as concentrated stocks at 20°C: leupeptin (10 mg/ml in ddH$_2$O), cycloheximide (2 mg/ml in ddH$_2$O), and brefeldin A (BFA; Epicentre, Madison WI; 5 mg/ml in ethanol). Final concentrations in experiments were as follows: 100 μM ALLN, 10 μM lactacystin, 20 μM ZL$_3$VS, 100 μg/ml leupeptin, 20 μg/ml cycloheximide, 200 μM chloroquine, and 6 μg/ml BFA.

Immunofluorescence Microscopy

Glass coverslips in 96-well dishes were treated with a solution of 0.5 mg/ml poly-D-lysine (Sigma; P7886) in 0.15 M boric acid, pH 8.4 for $\geq$30 min at 37°C and rinsed twice with PBS without Ca^{2+} and Mg^{2+}. PC12 transfectants were plated onto the coated coverslips and used for experiments after 4 d of culture, when ~75% confluent. For experiments at 37°C, the plating medium was replaced with fresh culture medium (with or without additions). Incubations at 20°C were conducted in Leibovitz's L15 medium (Life Technologies, Gaithersburg, MD; 11415-023) supplemented with 10% horse serum, 5% FCS, penicillin G, and streptomycin, in an ambient air (no CO$_2$)

refrigerator maintained at 20°C with a heating unit in a cold room as described in VanSlyke and Musil (2000).

At the time points specified in the figure legends, cells were rinsed three times with cold PBS (with Ca^{2+} and Mg^{2+}) before fixing with prechilled 2% paraformaldehyde in PBS for 30 min at room temperature. After fixation, cells were washed and then incubated in PBS for at least 30 min. Coverslips were incubated 30–60 min in blocking buffer (PBS plus 0.5% normal goat serum, 0.1% BSA, 0.2% Triton X-100, and 0.02% sodium azide) before addition of the desired primary antibody (or, in the case of double labeling, antibodies) diluted in blocking buffer. Hybridoma supernatant containing 7C6.C7 anti-Cx32 antibodies was used diluted 1:1. After an overnight incubation at 4°C in a humidified chamber, cells were incubated for 30 min in blocking buffer and then incubated with the appropriate secondary antibody for 1.5 h at room temperature followed by another 30-min rinse in blocking buffer. The coverslips were mounted onto glass slides with MOWIOL 4–88 mounting medium (Calbiochem, La Jolla, CA), and immunofluorescence images were captured using a Leica (Nussloch, Germany) DM LD photomicrography system and Scion (Frederick, MD) Image 1.60 software.

Metabolic Labeling

For metabolic labeling at 37°C, cells were first starved for methionine for 30 min at 37°C in Dulbecco's modified Eagle's medium lacking methionine supplemented with 5% dialyzed FCS and 2 mM glutamine ("labeling" medium). The medium was then replaced with fresh labeling medium containing [^{35}S]methionine (EXPRE^{35}S^{35}S; New England Nuclear, Boston, MA; 0.3 mCi/60-mm dish of cells, scaled proportionally for dishes of other sizes). For pulse–chase analysis, the radioactive medium was removed after a 30-min pulse and the cultures were rinsed once before addition of fresh complete culture medium supplemented with 0.5 mM nonlabeled methionine. For metabolic labeling at 20°C for analysis of Triton X-100 solubility (see Figure 3), cells in 60-mm dishes were incubated in 2.5 ml of reduced bicarbonate labeling medium (Earle's minimal essential medium lacking methionine and containing 15 mM HEPES, 0.35 g/l bicarbonate, 2 mM glutamine, and 5% dialyzed FCS) containing 0.3 mCi of [^{35}S]methionine at 37°C under ambient CO$_2$ conditions. For analysis of connexon assembly at 20°C (see Figure 8), cells in 60-mm dishes were first incubated in 2.5 ml of reduced bicarbonate labeling medium for 30 min at 37°C under ambient CO$_2$ conditions. The medium was replaced with 2.5 ml of fresh reduced bicarbonate labeling medium containing 0.3 mCi of [^{35}S]methionine, and the cells were incubated at 37°C for 20 min under the same conditions before chilling the tissue culture dish briefly to 4°C and continuing the labeling for an additional 4 h 40 min in a 20°C ambient CO$_2$ incubator (VanSlyke and Musil, 2000). The initial 20 min of labeling at 37°C increases the amount of radiolabeled connexin synthesized but is too short to permit detectable assembly of wild-type Cx32 into Triton X-100-insoluble gap junctional plaques.

Immunoprecipitation

With the exception of cells to be lysed under nondenaturing conditions in Triton X-100 (see below), cells were rinsed once with PBS at 4°C and resuspended in lysis buffer (5 mM Tris base, 5 mM EDTA, 5 mM EGTA, 10 mM iodoacetamide, and 2 mM PMSF, pH 8.0) supplemented with 0.6% SDS, 250 μg/ml soybean trypsin inhibitor, and 200 μM leupeptin. The lysates were then immunoprecipitated with the desired antibody as described by Le and Musil (1998). Two modifications were made for immunoprecipitation of Cx32: first, cells were lysed in SDS at room temperature for 30 min instead of at 100°C for 3 min to minimize aggregation of Cx32; and second, samples were precleared with protein A-Sepharose for 2 h at 4°C before addition of anti-Cx32 antibody (VanSlyke and Musil, 2000).

Triton X-100 Solubilization and Chemical Cross-Linking

Metabolically labeled tissue culture cells were resuspended in incubation buffer (136.8 mM NaCl, 5.36 mM KCl, 0.336 mM Na$_2$HPO$_4$, 0.345 mM KH$_2$PO$_4$, 0.8 mM MgSO$_4$, 2.7 mM CaCl$_2$, and 20 mM HEPES, pH 7.5) and solubilized in the presence of 1% Triton X-100 on ice for 30 min as previously described (Musil and Goodenough, 1993). The cell extract was separated into Triton X-100-insoluble and -soluble fractions by centrifugation at $100,000 \times g$ (45,000 rpm in a TLA100.3 tabletop ultracentrifuge; Beckman Instruments, Palo Alto, CA) for 50 min at 4°C. For analysis of Cx32 Triton X-100 solubility (see Figure 3), each fraction was lysed in SDS and immunoprecipitated as described for Cx43 (Musil and Goodenough, 1991), except that the samples were lysed in SDS at room temperature for 30 min and precleared with protein A-Sepharose as described above. For cross-linking analysis of Cx32 connexons, the Triton X-100-soluble fraction was incubated for 30 min on ice with 1 mM ethylene glycolbis(succinimdylsuccinate) (EGS; Pierce), freshly diluted from a 100 mM stock in DMSO. The cross-linking reaction was stopped by addition of glycine as detailed by Musil and Goodenough (1993), SDS was added to a final concentration of 0.6%, and the sample was incubated for 30 min at room temperature before immunoprecipitation of Cx32 as described above. Mock cross-linked control samples were treated identically but received DMSO only.

SDS-PAGE and Quantification

Monomeric Cx32, Cx43, and L-CAM immunoprecipitates were analyzed on 11, 10, or 7.5% SDS-PAGE gels, respectively, after incubation of samples in SDS-PAGE sample loading buffer for either 30 min at room temperature (Cx32) or for 3 min at 100°C (Cx43 and L-CAM). Samples containing cross-linked Cx32 were warmed to 37°C for 5 min before analysis on 7.5–12.5% gradient gels. The dried gels were quantitated on a 445 SI PhosphorImager (Molecular Dynamics, Sunnyvale, CA) using IPLab Gel software (Signal Analytics, Vienna, VA).

RESULTS

Intracellular Localization of the R142W, E186K, and E208K CMTX-linked Cx32 Mutants in PC12 Cell Transfectants

We examined three CMTX-linked Cx32 point mutants reported by Deschenes *et al.* (1997) to be associated with moderate to severe clinical disease. The R142W mutation converts arginine 142 to a tryptophan in a position within the third transmembrane domain of Cx32 that is occupied by a basic residue in all known members of the connexin family and that is thought to contribute to the gap junction channel pore. The E186K mutation changes the charge of an amino acid at the end of the second extracellular loop that is perfectly conserved within the connexin family, whereas the E208K mutation similarly reverses the polarity of another perfectly conserved glutamic acid residue that borders the last transmembrane domain. These mutants have been reported to be nonfunctional when expressed in paired *Xenopus* oocytes (Bruzzone *et al.*, 1994; Castro *et al.*, 1999).

Figure 1 shows the steady-state localization of these mutants and WT Cx32 when stably expressed in otherwise connexin-deficient PC12 transfectants. WT Cx32 accumulated on the cell surface and concentrated at cell–cell interfaces in the punctate distribution characteristic of gap junctional plaques (Figure 1A; also see Figure 5A). As previously reported (Deschenes *et al.*, 1997), the R142W, E186K, and E208K Cx32 mutants instead were localized by immunoflu-
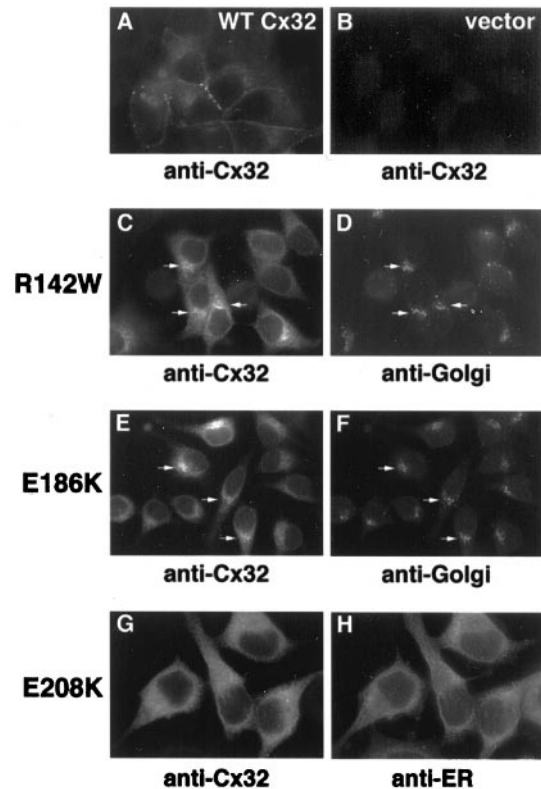

Figure 1. Steady-state intracellular localization of WT Cx32 and CMTX-linked Cx32 mutants. PC12 cell lines expressing WT Cx32 (A), R142W Cx32 (C and D), E186K Cx32 (E and F), or E208K Cx32 (G and H) or transfected with vector only (B) were fixed and immunostained with anti-Cx32 antibodies (A, C, E, and G). Cells expressing CMTX-linked Cx32 mutants were doubly immunostained for markers specific for either the *cis/medial*-Golgi (mannosidase II; D and F) or the ER (calreticulin; H). Arrows (C–F) point to Golgi regions doubly stained for Cx32 and mannosidase II.

orescence microscopy exclusively intracellularly in multiple independent clones (Figure 1; also see Figure 5). They were also undetectable on the plasma membrane by cell surface biotinylation (our unpublished data). Accumulation of immunodetectable E208K, R142W, or E186K Cx32 on the cell surface could not be induced by incubating the cells for 48 h at either 25 or 27°C (our unpublished data). The trafficking defect of these mutants is therefore distinct from that of the ΔF508 form of the cystic fibrosis transmembrane conductance regulator (CFTR), which is retained within the ER at 37°C but is transported to the cell surface at lower temperatures (Denning *et al.*, 1992).

Double-staining immunofluorescence microscopy studies revealed differences in the subcellular localization of the CMTX-linked Cx32 mutants. E208K Cx32 showed nearly perfect colocalization with an ER marker (calreticulin) in a distribution readily distinguishable from that obtained with a Golgi resident (mannosidase II) (Figure 1). In each of the E208K Cx32-expressing PC12 clonal cell lines we have examined, the perinuclear, Golgi-like staining pattern described by Deschenes *et al.* (1997) in a minority of highly expressing cells was not observed. Possibly, such transfec-

tants were selected out of the population during repeated passage. The intracellular localization of E208K Cx32 was unaffected by treatments that accumulate newly synthesized, transport-competent secretory proteins within either the peripheral elements of the intermediate compartment or the Golgi apparatus (16°C, nocodazole; 20°C, monensin) (Matlin and Simons, 1983; Hsu *et al.*, 1991; Jackson *et al.*, 1993; our unpublished results). The E186K and R142W Cx32 mutants could also be detected within the ER. In contrast to E208K Cx32, however, their staining pattern was not restricted to this organelle but instead included Golgi-like perinuclear compartments where they colocalized with mannosidase II. These findings suggest that E208K Cx32 remains confined to the ER, whereas the R142W and E186K mutants are competent to traffic to more distal compartments of the secretory pathway but not to the cell surface.

Rapid Turnover of WT and Mutant Cx32 in PC12 Cells

As defined by Aridor and Balch (1999), class II mutations are distinguished from class I defects in that they inhibit not only the intracellular transport but also the degradation of the affected protein, leading to deleterious overaccumulation within the early secretory pathway. Reduced turnover of disease-causing mutants of both soluble and integral plasma membrane proteins has been recapitulated in tissue culture cell systems (Graham *et al.*, 1990; Sadeghi *et al.*, 1997; Skovronsky *et al.*, 1998). In some (but not all) cases, both the trafficking and degradation defects of class II mutants are associated with polymerization of the affected protein in aggregates insoluble in the nonionic detergent Triton X-100 (Graham *et al.*, 1990; Kim and Arvan, 1998; Skovronsky *et al.*, 1998). To investigate whether the E208K, R142W, and E186K Cx32 mutants behave like class I or class II mutants in PC12 transfectants, we examined their rate of turnover (Figure 2) and detergent sensitivity (Figure 3). Less than 30% of WT Cx32 metabolically labeled with [35S]methionine during a 30-min pulse was immunoprecipitable after a 4-h chase, as expected from the rapid rate of degradation typical of Cx32 and other members of the connexin family in cultured cells as well as in vivo (Fallon and Goodenough, 1981; Musil *et al.*, 1990; Beardslee *et al.*, 1998). As assessed by pulse–chase analysis, each of the three CMTX-linked Cx32 mutants tested was degraded at least as rapidly as the wild-type protein (Figure 2), whereas a [35S]methionine-labeled, metabolically stable cellular protein (actin) was not detectably turned over during the same period (our unpublished data). To assess the detergent solubility of WT and mutant forms of Cx32, PC12 transfectants labeled for 4 h with [35S]methionine were lysed in 1.0% Triton X-100 at 4°C (Figure 3). Previous studies have demonstrated that newly synthesized WT Cx43 is soluble under these conditions and acquires resistance to Triton X-100 only upon incorporation into gap junctional plaques (Musil and Goodenough, 1991). We show here that WT Cx32 has similar properties. [35S]methionine-labeled Cx32 endogenously expressed in MH_1C_1 hepatoma cells was essentially completely (>96%) Triton soluble when metabolically labeled at 20°C, a temperature at which transport to the plasma membrane and therefore formation of gap junctional plaques are inhibited (Matlin
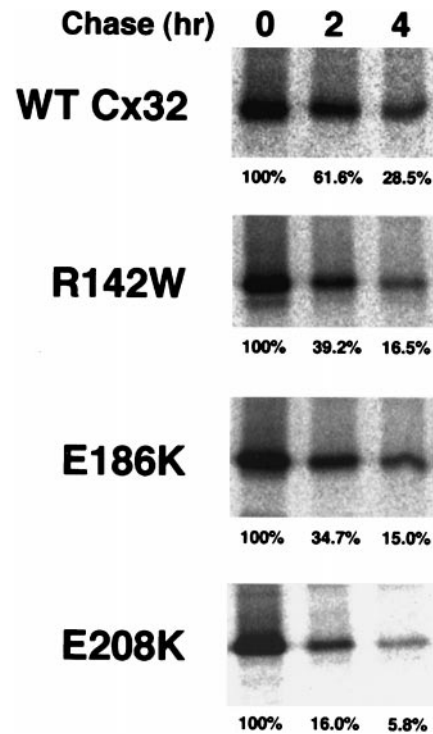

Figure 2. Pulse–chase analysis of the turnover of WT Cx32 and CMTX-linked mutants. PC12 transfectants were metabolically labeled with [35S]methionine for 30 min at 37°C and then chased in the presence of excess cold methionine for 0, 2, or 4 h. Cx32 was immunoprecipitated from equal volumes of total cell lysate (and therefore from equal numbers of cell equivalents) and analyzed by SDS-PAGE. The amount of [35S]methionine-Cx32 recovered by immunoprecipitation after each chase period was expressed as a percentage of [35S]methionine-Cx32 immunoprecipitable immediately after the pulse.

and Simons, 1983). In contrast, a considerable amount (45%) of [35S]methionine-labeled Cx32 synthesized at 37°C was insensitive to Triton X-100. Given the well-known insolubility of Cx32 gap junctional plaques in most nonionic detergents (Hertzberg, 1984), the acquisition of Triton X-100 resistance of Cx32 in MH_1C_1 cells at 37°C is likely to be due to gap junction assembly. WT Cx32 expressed in PC12 cells showed a comparable temperature dependence in its response to Triton X-100, in keeping with their ability to form gap junctional plaques. In contrast, each of the three CMTX-linked Cx32 mutants examined could be almost completely (>95%) solubilized by Triton X-100 when synthesized at 37°C. Examination of the total cellular pool of mutant Cx32 by Western blotting also failed to provide evidence of accumulation in stable high-molecular-weight aggregates (our unpublished results). The R142W, E186K, and E208K forms of Cx32 therefore behave differently than the PiZ mutant of α_1-antitrypsin, of which a fraction too small to be detectable by short-term metabolic labeling slowly accumulates in degradation-resistant, Triton X-100-insoluble aggregates that over time become the predominant cellular form of the protein as assessed by immunoblotting (Graham *et al.*, 1990).
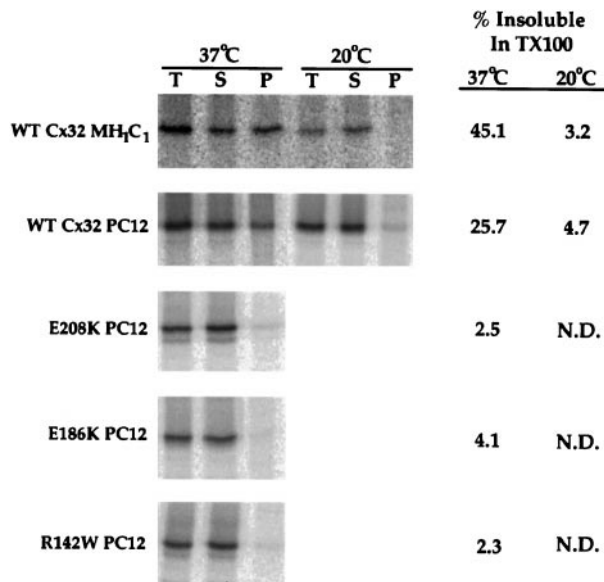
Figure 3. Solubility of WT Cx32 and CMTX-linked mutants in Triton X-100. Cx32-expressing cells were metabolically labeled with [^{35}S]methionine for either 4 h at 37°C or 5 h at 20°C. Cells were lysed in 1% Triton X-100 at 4°C and subjected to centrifugation at 100,000 × *g* for 50 min. Cx32 was immunoprecipitated from the total extract (T), Triton X-100-soluble supernatant (S), and Triton X-100-insoluble pellet (P) and analyzed by SDS-PAGE. In all cases, recovery of radiolabeled Cx32 (S + P/T) was ≥93%. N.D., not determined.

Pathways of WT Cx32 Degradation

The rapidity with which both WT and mutant forms of Cx32 are turned over despite their disparate subcellular localizations raised the question of whether they were degraded by the same or distinct mechanisms. To examine this issue, we treated PC12 cell transfectants with inhibitors of either the lysosome or the proteasome, the two major pathways implicated in the destruction of integral plasma membrane proteins (Seglen, 1983; Lee and Goldberg, 1998).

We first investigated the mechanism(s) by which WT Cx32 is degraded by pulse–chase analysis (Figure 4). To inhibit lysosomal degradation, we used the tripeptide leupeptin instead of a weak base to avoid the potentially confounding effect of the latter on Golgi intracisternal pH and function (Seglen, 1983; Stevens and Forgac, 1997). Addition of leupeptin to the chase medium modestly but reproducibly increased the amount of pulse-labeled Cx32 that survived a 6-h chase by ~1.5-fold. A much greater inhibition of degradation was achieved in the presence of the proteasome inhibitor ALLN (Figure 4). In a more limited series of experiments, a mechanistically distinct, highly selective blocker of the proteasome (ZL$_3$VS) had a comparable effect, increasing the amount of pulse-labeled [^{35}S]methionine-WT Cx32 that survived a 6-h chase an average of 2.3-fold (±0.35; *n*=3). The relative efficacy of proteasomal and lysosomal inhibitors in slowing WT Cx32 turnover is very similar to that previously reported by Laing and Beyer (1995) for WT Cx43 endogenously expressed in a CHO cell subclone.

The role of lysosomes in the turnover of at least a fraction of WT Cx32 molecules was corroborated by immunofluores-
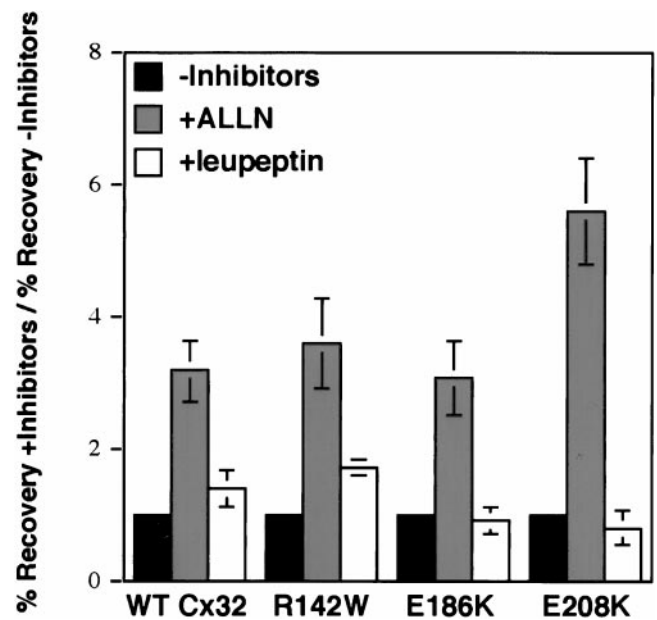

Figure 4. Pulse–chase analysis of degradation of WT Cx32 and CMTX-linked Cx32 mutants. PC12 cell transfectants were metabolically labeled for 30 min with [^{35}S]methionine and then chased at 37°C for 6 h in either the absence or presence of 100 μM ALLN or 100 μg/ml leupeptin. Cx32 was immunoprecipitated from equal volumes of total cell lysate (and therefore from equal numbers of cell equivalents) and analyzed by SDS-PAGE. The data are presented as the fold increase in the percent recovery of Cx32 after a 6-h chase in the presence of inhibitors relative to the percent recovery of Cx32 in the absence of inhibitors.

cence microscopy (Figure 5). Unlike leupeptin, weak bases such as chloroquine inactivate proteases within endosomes and lysosomes by neutralizing lumenal pH. A consequence of this activity is osmotic swelling of these compartments into characteristic "doughnut" structures that are morphologically distinct from the Golgi and other normally acidic organelles (Mellman *et al.*, 1986). WT Cx32 could be readily detected in such distended vesicles after a 3- to 6-h incubation of cells with 200 μM chloroquine (Figure 5C). In contrast, proteasome inhibitors including ALLN (Figure 5B) and ZL$_3$VS (our unpublished results) did not detectably change the pattern of WT Cx32 staining.

Proteasome inhibitor-sensitive degradation of integral plasma membrane proteins has been reported to occur before their exit from the ER and/or after their transport to the cell surface (reviewed by Bonifacino and Weissman, 1998). Although evidence that WT Cx43 may be subjected to proteasomal degradation at the latter site has been reported by Laing *et al.* (1997), it is unknown whether this process is also involved in connexin turnover at earlier stages of the secretory pathway. Connexins are not glycosylated or known to undergo any other type of post-translational modification that could be used to biochemically monitor their transport through the cell. The extent of proteasome inhibitor-sensitive turnover of WT Cx32 in the ER was therefore assessed by conducting pulse–chase experiments in the presence of BFA, which blocks the vesicular export of newly synthesized proteins from this compartment (Klausner *et al.*, 1992) (Fig-
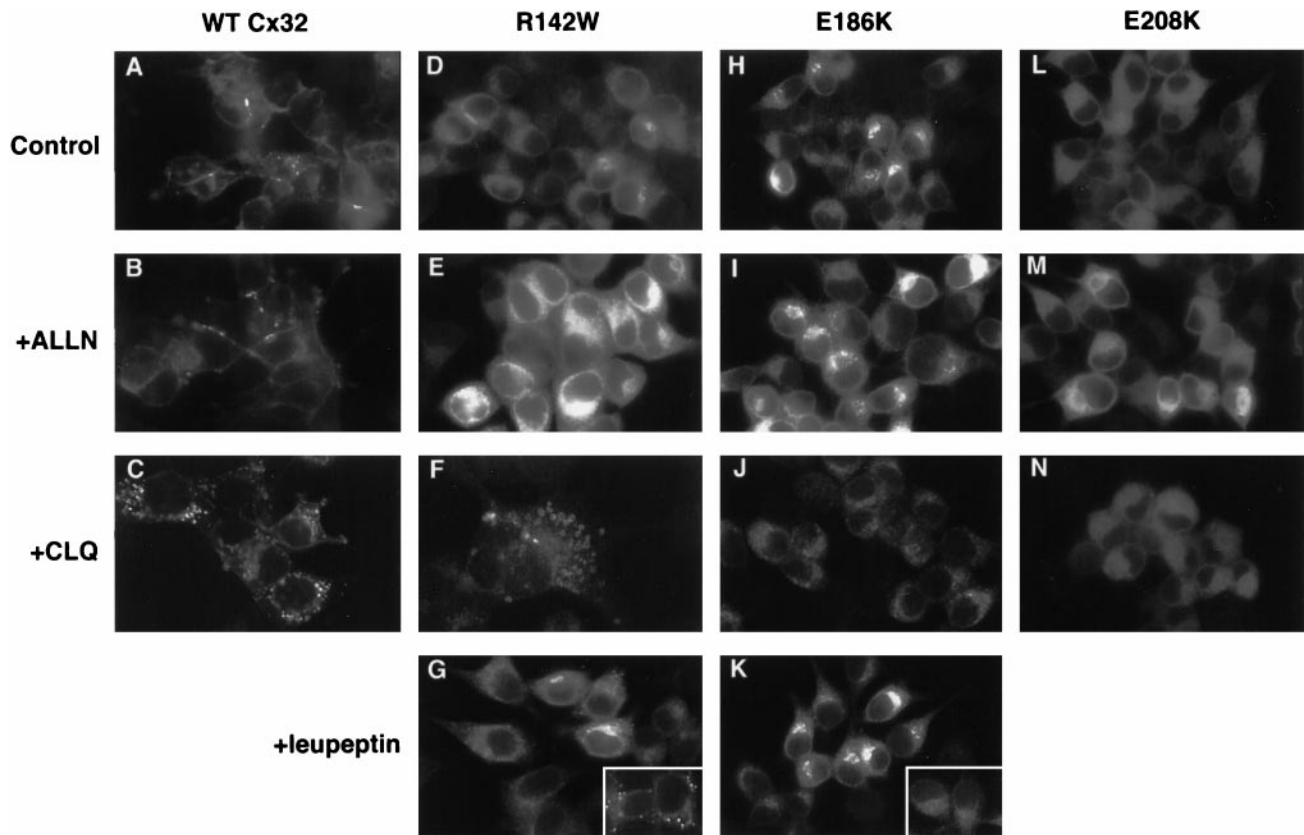
Figure 5. Effect of lysosomal and proteasomal inhibitors on WT and mutant Cx32 immunostaining. PC12 cell transfectants expressing WT Cx32 (A–C), R142W Cx32 (D–G), E186K Cx32 (H–K), or E208K Cx32 (L–N) were stained for Cx32 after incubation for 6 h at 37°C with medium alone (A, D, H, and L), 100 μM ALLN (B, E, I, and M), 200 μM chloroquine (C, F, J, and N), or 100 μg/ml leupeptin (G and K). Insets in G and K, cells were chased with 20 μg/ml cycloheximide in the presence of 100 μg/ml leupeptin for 3.5 h at 37°C.

ure 6). To examine only the initial stages of connexin degradation, and because connexins might become subject to additional, physiologically irrelevant proteolytic pathways during prolonged exposure to BFA, we labeled cells for only 30 min and limited our analysis to a 2- to 3-h chase. During this period, BFA did not slow the degradation of WT Cx32 in PC12 cell transfectants. Turnover of WT Cx32 in either the absence or presence of BFA was efficiently inhibited by the proteasome inhibitor ALLN. BFA also had very little effect on the degradation of endogenously expressed WT Cx32 in MH_1C_1 cells or WT Cx43 in CHO, normal rat kidney, L929, or primary lens epithelial cells (CHO data shown in Figure 6). In all cell types examined, general ER–Golgi trafficking was sensitive to BFA as verified by redistribution of mannosidase II into the ER (our unpublished results). Rapid, proteasome-mediated degradation in the ER is therefore not limited to a single connexin species or an artifact of exogenous connexin expression. Control experiments demonstrated that BFA strongly inhibited the otherwise rapid ($t_{1/2}$ ~3 h) degradation of the connexin-unrelated integral plasma membrane protein L-CAM (Figure 6), demonstrating that ER degradation is not a general consequence of BFA treatment but instead reflects a specific property of connexins.

Pathways of Mutant Cx32 Degradation

Having examined the role of the lysosome and proteasome in WT Cx32 turnover, we next investigated the involvement of these pathways in the degradation of the E208K, R142W, and E186K CMTX-linked Cx32 forms. Pulse–chase analysis revealed that all three mutants were as sensitive to the proteasome inhibitor ALLN as the wild-type protein (Figure 4). The lysosomal inhibitor leupeptin enhanced the recovery of the R142W mutant to about the same extent as it did WT Cx32 but did not influence the turnover of E208K Cx32, in keeping with the exclusively ER immunolocalization pattern of the latter mutant at steady state (Figure 1). Surprisingly, leupeptin also had no detectable effect on the turnover of the E186K Cx32 mutant despite its ability to traffic to post-ER compartments.

Participation of the lysosome in the degradation of R142W Cx32, but not of the E186K or E208K mutants, was supported by immunolocalization studies (Figure 5). Similar to its effect on WT Cx32, chloroquine treatment of R142W Cx32-expressing cells caused some of the mutant molecules to accumulate in swollen vesicles with the characteristic doughnut-like morphology taken on by components of the endosome–lysosome system in the presence of this lysosomotropic amine (Figure 5F). In contrast, neither the E186K
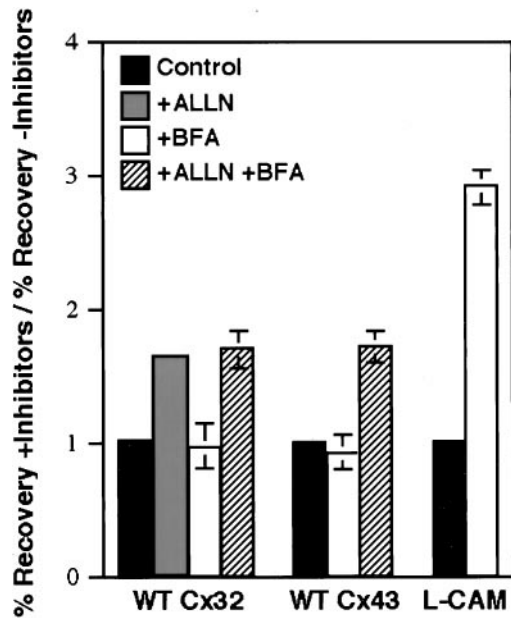
Figure 6. Degradation of wild-type connexins retained within the ER. WT Cx32-expressing PC12 cell transfectants, CHO cells endogenously expressing WT Cx43, and L-CAM-expressing S180L cells were pulse-labeled for 30 min with [^{35}S]methionine in the absence or presence of 6 μg/ml BFA. Cells were then chased (with or without BFA) for 2, 3, or 6 h, respectively. BFA causes retention of newly synthesized proteins within the ER. Where indicated, 100 μM ALLN was included in the chase medium. The data are presented as the fold increase in the percent recovery of pulse-labeled protein (Cx32, Cx43, or L-CAM) after the chase period in the presence of inhibitor(s) relative to the percent recovery of pulse-labeled protein in the absence of inhibitor. Recovery after chase in the absence of inhibitors (control) averaged 56% for WT Cx32 and 60% for WT Cx43. Complete inhibition of Cx degradation (=100% recovery) therefore corresponds to a 1.8-fold increase in recovery of WT Cx32 and a 1.7-fold increase in recovery of WT Cx43, very close to the values obtained in the presence of ALLN either with or without BFA. For each experimental condition, n = 3.

(Figure 5J) nor the E208K (Figure 5N) Cx32 mutant was detected in such distended vesicles after chloroquine exposure. R142W Cx32 (Figure 5G), but not the E186K species (Figure 5K), could also be observed in lysosome-like punctate structures after treatment of cells with leupeptin. Because leupeptin does not cause vacuolar swelling, staining of R142W Cx32 in the endosome–lysosome system was often not obvious above anti-Cx32-immunoreactivity in the ER but became readily detectable if cycloheximide was used to chase preexisting Cx32 into post-ER compartments (Figure 5G, inset). The proteasome inhibitor ALLN increased the intensity but did not change the pattern of staining of the R142W, E186K, or E208K Cx32 species (Figure 5, E, I, and M). The transport defects of these mutants therefore cannot be overcome by reducing their proteasomal turnover.

Although successfully used to assess the role of the proteasome in the turnover of a wide variety of proteins, ALLN also inhibits certain lysosomal cathepsins as well as calpains (Lee and Goldberg, 1998). To rule out the possibility that the effect of ALLN on the degradation of the Cx32 mutants was
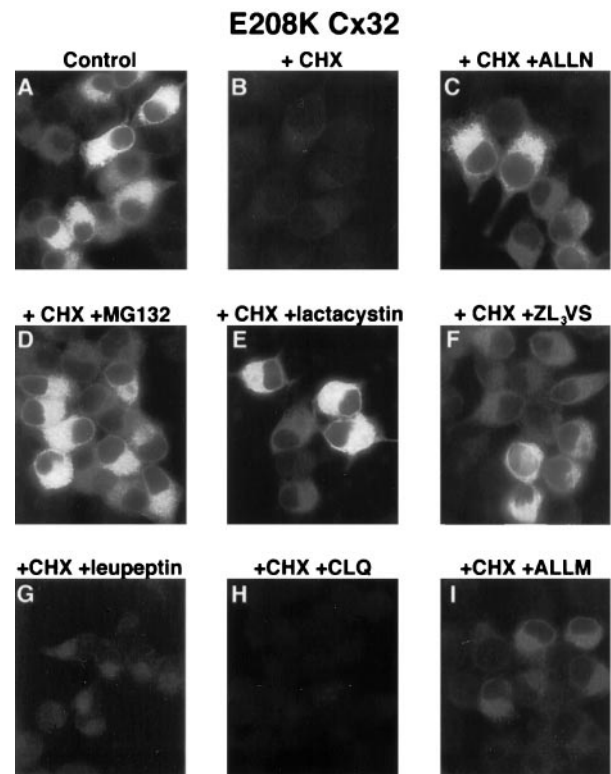
E208K Cx32

Figure 7. Effect of lysosomal and proteasomal inhibitors on E208K Cx32 degradation. E208K Cx32-expressing cells were incubated for 6 h at 37°C in either the absence (A) or presence (B–I) of 20 μg/ml cycloheximide with the following additions: 100 μM ALLN (C), 20 μM Cbz-leu-leu-leucinal (D), 10 μM lactacystin (E), 20 μM ZL$_3$VS (F), 100 μg/ml leupeptin (G), 200 μM chloroquine (H), or 100 μM ALLM (I).

due to nonproteasomal activity of the drug, we conducted immunocytochemical studies using the protein synthesis blocker cycloheximide. Control experiments demonstrated that 20 μg/ml cycloheximide effectively inhibited incorporation of [^{35}S]methionine into nascent proteins within 10 min and did not alter the rate of degradation of previously synthesized [^{35}S]methionine-labeled E208K Cx32, R142W Cx32, or E186K Cx32 (our unpublished results). Incubation of cells expressing these mutants with cycloheximide for 6 h resulted in the almost complete loss of anti-Cx32 immunoreactivity, in keeping with their rapid rate of degradation. As expected from pulse–chase analysis (Figure 4), the disappearance of mutant staining in cycloheximide-treated cells was largely prevented by ALLN (data for E208K Cx32 shown in Figure 7 and for E186K Cx32 in Figure 8). Similar results were obtained with the related proteasome inhibitor Cbz-leu-leu-leucinal as well as with two highly selective, mechanistically distinct blockers of proteasomal proteolysis, ZL$_3$VS and lactacystin (data for E208K Cx32 shown in Figure 7). The specificity of this effect for proteasomal inhibitors was demonstrated using the E208K Cx32 mutant, which in pulse–chase experiments was shown to be insensitive to leupeptin (Figure 4). Neither leupeptin (Figure 7G) nor the mechanistically unrelated lysosomal inhibitor chloroquine (Figure 7H) was able to prevent the loss of immunologically
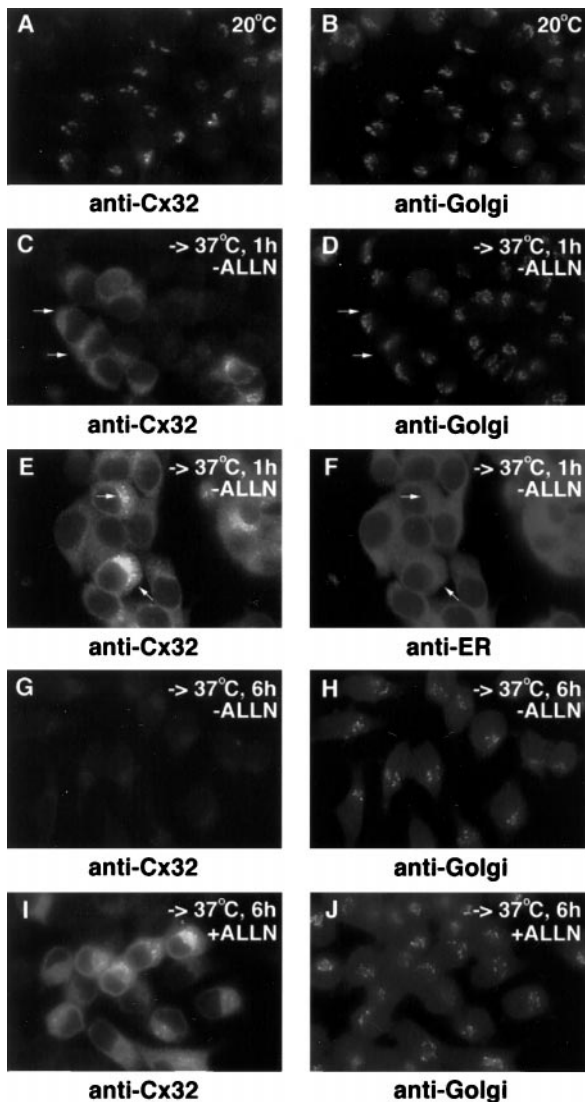
Figure 8. Retrograde transport of E186K Cx32. E186K Cx32-expressing PC12 cell transfectants were incubated at 20°C for 3 h and then either fixed immediately (A and B) or shifted to 37°C in the presence of 20 μg/ml cycloheximide. The latter cells were incubated at 37°C for either 1 h (C–F) or 6 h (G and H) in the absence of further additions or for 6 h in the presence of 100 μM ALLN (I and J). All cells were immunostained for Cx32 and in some cases doubly stained for the *cis/medial*-Golgi (mannosidase II; B, D, H, and J) or the ER (calreticulin; F). Arrows in C and D point to regions that stain for Cx32 but not mannosidase II; arrows in E and F indicate areas of colocalization of Cx32 and calreticulin.

detectable E208K Cx32 in cycloheximide-treated cells. Furthermore, ALLM, closely related to ALLN and an effective blocker of calpains and cathepsins but not of the proteasome (Rock *et al.*, 1994), had a much weaker effect on E208K Cx32 recovery than did ALLN, lactacystin, or ZL$_3$VS (Figure 7I). Although comparable experiments were not possible with WT Cx32 because of the fact that cycloheximide itself strongly inhibits degradation of wild-type forms of both
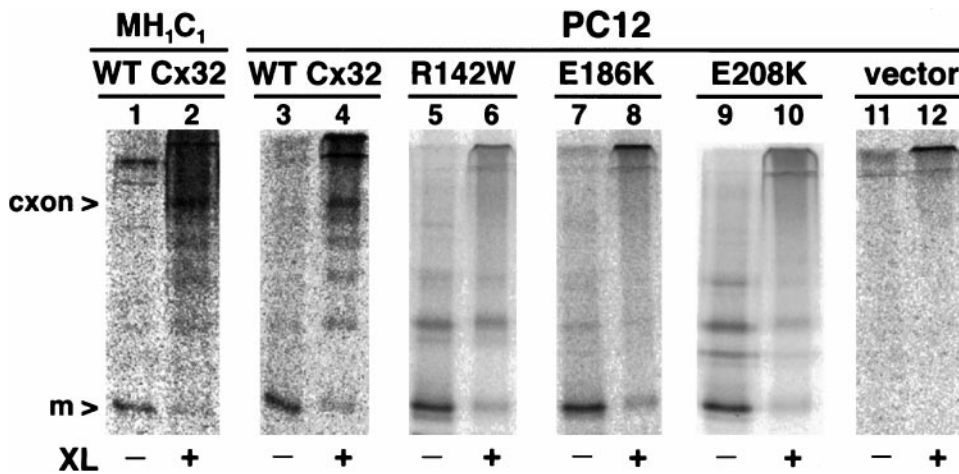
Cx32 and Cx43 (L.S. Musil, unpublished results), the aforementioned ability of ZL$_3$VS to reduce WT Cx32 turnover in pulse–chase experiments strongly supports a role for the proteasome in the turnover of this species as well.

E186K Cx32 Undergoes Retrograde Transport Back to the ER

Proteasome-mediated degradation in the early secretory pathway requires that the substrate protein, in either an intact or partially degraded state, be extracted from membranes and inserted into cytosolic proteasomes (reviewed by Plemper and Wolf, 1999). To date, the ER is the only intracellular site at which this "dislocation" process has been reported to occur. Given that E186K Cx32 does not enter the endosome–lysosome system or traffic to the cell surface, the question arises of how this mutant is degraded from post-ER compartments. To address this issue, we took advantage of the serendipitous observation that a 3-h incubation of living cells at 20°C caused E186K Cx32 to concentrate very strongly within the Golgi region (Figure 8A). To study the fate of this post-ER pool of E186K Cx32, we returned cells to 37°C in the presence of cycloheximide to inhibit new protein synthesis. Beginning at ~10 min after warm-up, the perinuclear staining pattern of the mutant was gradually replaced by a more diffuse, reticular distribution that was most striking 30–50 min later (Figure 8, C and E). Double-staining immunofluorescence microscopy demonstrated that the mutant now colocalized predominantly with the ER marker calreticulin (Figure 8F) instead of with mannosidase II (Figure 8D), indicating that it had undergone retrograde transport back into the ER. This interpretation is in keeping with previous data suggesting that Golgi-to-ER transport is inhibited to a greater extent at 20°C than anterograde ER-to-Golgi movement, leading to a relative accumulation of transport-competent proteins in the Golgi at 20°C that is reversed upon return to 37°C (Hsu *et al.*, 1991; Cole *et al.*, 1996). Immunodetectable E186K Cx32 disappeared over the next 5 h (Figure 8G), as expected from its rapid rate of turnover in either the absence (Figure 2) or presence (our unpublished results) of cycloheximide as determined by pulse–chase analysis. Degradation of E186K Cx32 over the same period, but not its retrograde transport to the ER, was blocked by the proteasome inhibitor ALLN (Figure 8I). Taken together with the data in Figures 4 and 5, these results indicate that E186K Cx32 is turned over by a proteasome-mediated pathway even after its initial exit from the ER. Degradation of such post-ER pools of E186K Cx32 may require retrieval back into the endoplasmic reticulum, from which it might access the proteasome via the translocon channel.

Effect of CMTX-linked Cx32 Mutations on Connexon Assembly

The first step in gap junction formation is the noncovalent assembly of six connexin monomers into a connexon before transport to the cell surface. It has been suggested that the ability of intracellularly retained CMTX-linked Cx32 mutants to act as dominant negative inhibitors of WT connexins is due to the formation of mixed connexons (Omori *et al.*, 1996; Deschenes *et al.*, 1997). To assess the competence of the R142W, E186K, and E208K Cx32 mutants to undergo connexon assembly, we assayed their oligomerization state

Figure 9. CMTX-linked Cx32 mutants do not assemble connexons. PC12 cells expressing WT Cx32 (lanes 3 and 4), mutant Cx32 (lanes 5–10), or no Cx32 (lanes 11 and 12) were metabolically labeled for 20 min at 37°C and then 4.6 h at 20°C as described in MATERIALS AND METHODS. Alternatively, MH$_1$C$_1$ cells (lanes 1 and 2) were labeled for 4 h at 37°C. Triton X-100-solubilized cell extracts were cross-linked with 1 mM EGS for 30 min at 4°C (lanes 2, 4, 6, 8, 10, and 12), or treated with DMSO only for a mock–cross-linked control (lanes 1, 3, 5, 7, 9, and 11). Cx32 was immunoprecipitated and analyzed by SDS-PAGE on 7.5–12.5% gradient gels. The positions of monomeric Cx32 (m) and cross-linked Cx32 connexons (cxon) are indicated at the left. The bands migrating slower than monomeric Cx32 in non–cross-linked mutant immunoprecipitates are mainly SDS-induced aggregates of Cx32.

when expressed individually in PC12 cell transfectants (Figure 9). We first verified that assembly of WT Cx32 into connexons could be detected using techniques previously established for Cx43 (Musil and Goodenough, 1993). Cells were metabolically labeled with [^{35}S]methionine and then lysed in the presence of Triton X-100 at 4°C before cross-linking of the soluble fraction with EGS and analysis of Cx32 oligomers by immunoprecipitation and SDS-PAGE. As expected, WT Cx32 in PC12 transfectants could be cross-linked to an ~150-kDa species indistinguishable from Cx32-containing connexons isolated from MH$_1$C$_1$ cells (Figure 9, lanes 2 and 4) or rat liver (our unpublished results; Cascio *et al.*, 1995). In contrast, none of the three mutants could be cross-linked into a detectable connexon species (Figure 9, lanes 6, 8, and 10) despite expression levels roughly equivalent to (E186K and R142W) or somewhat greater than (E208K) that of WT Cx32. Similar results were obtained if cells were labeled at 37°C in the presence of ALLN to reduce the rate of connexin degradation (our unpublished results), indicating that rapid turnover is not responsible for the inability of the mutants to assemble into connexons.

DISCUSSION

Although defects in the Cx32 gene were identified as the cause of CMTX disease more than 7 years ago (Bergoffen *et al.*, 1993), the mechanism(s) by which these mutations lead to peripheral nerve pathology have not been deliniated. In this study we have examined the assembly, trafficking, and degradation of three CMTX-linked Cx32 point mutants stably expressed in PC12 cell transfectants. The E208K, R142W, and E186K Cx32 mutants were undetectable on the cell surface by either morphological (immunofluorescence microscopy) or biochemical (cell surface biotinylation) assays. Insofar as oligomeric assembly is a general prerequisite for the trafficking of multisubunit proteins to the cell surface (Hammond and Helenius, 1995), the inability of these mutants to form connexons is also consistent with their intracellular retention. Two major conclusions arise from our findings and are discussed below. First, the E208K, R142W,

and E186K Cx32 mutations are unlikely to cause CMTX by accumulating in poorly degradable intracellular aggregates. Second, each of these mutants has a distinct intracellular trafficking and degradative fate, revealing a multistep quality control mechanism that prevents abnormal connexins from being transported to the plasma membrane.

Implications for the Mechanism of CMTX Disease

By definition, mutations that prevent the transport of a plasma membrane protein to the cell surface cause the loss of the protein's wild-type function. As described by Aridor and Balch (1999), class I mutations result in the efficient degradation of the affected secretory protein at the level of the ER by a proteasome-mediated process. Class II mutations inhibit the protein's turnover as well as its intracellular transport, resulting in chronic, pathological activation of ER stress responses and in some cases misfolding of the accumulated mutant protein into Triton X-100-insoluble aggregates (Kim and Arvan, 1998; Aridor and Balch, 1999). Three lines of evidence indicate that the E208K, R142W, and E186K CMTX-linked forms of Cx32 behave as class I instead of class II mutants in PC12 cell transfectants. First, pulse–chase analysis revealed that all three mutants, like wild-type connexins, were degraded at a rapid rate (Figure 2). Inhibition of new protein synthesis with cycloheximide resulted in the loss of all immunofluorescently detectable E186K Cx32 (Figure 8) as well as E208K (Figure 7) and R142W Cx32 (our unpublished results) within a 6-h period, indicating that fast turnover is a property of the total cellular pool of mutant Cx32 and not just the fraction that incorporates [^{35}S]methionine during a 30-min pulse. Second, ALLN and lactacystin inhibited the degradation of all three mutants within the early secretory pathway, implicating the proteasome in their destruction. Third, the mutants were soluble in 4°C Triton X-100 as detected by either immunoprecipitation after a 4-h labeling (>twice the t$_{1/2}$ of the protein) (Figure 3) or by Western blotting (our unpublished results), in contrast to certain abnormal proteins that form toxic aggregates (Graham *et al.*, 1990; Skovronsky *et al.*, 1998; Greenfield *et al.*,

1999). Our findings in PC12 cells are consistant with the observation (L. Bone, A. Messing, R. Balice-Gordon, K. Fischbeck, and S. Scherer, unpublished observation) that the ER and Golgi compartments of Schwann cells of transgenic mice expressing the R142W Cx32 mutant appear normal instead of taking on the distended morphology characteristic of class II disorders and their murine models, including Pelizaeus–Merzbacher disease (Gow and Lazzarini, 1996), α_1-anti-trypsin deficiency (Carlson *et al.*, 1989), and congenital hypothyroid goiter (Mayerhofer *et al.*, 1988; Aridor and Balch, 1999).

The absence of evidence of intracellular accumulation of CMTX-linked Cx32 mutants does not, however, mandate that they act as simple nulls. Several such mutants, including E186K and R142W Cx32, have been shown to inhibit the function of coexpressed WT Cx32 in paired *Xenopus* oocytes (Bruzzone *et al.*, 1994), transfected tissue culture cells (Omori *et al.*, 1996), and/or (in the case of R142W Cx32) transgenic mice (Scherer *et al.*, 1999). Bruzzone *et al.* (1994) have demonstrated that E186K and R142W Cx32 also block the activity of certain other, but not all, connexin family members. Because the Cx32 gene is subject to X inactivation (Scherer *et al.*, 1998), WT and mutant forms of Cx32 do not coexist within the same cell in CMTX patients. Any physiologically relevant interaction must therefore be between mutant Cx32 and a non-Cx32 connexin. Evidence for the existence of other connexin species in myelinating Schwann cells has recently been provided by Balice-Gordon *et al.* (1998), who demonstrated the continued presence of a radial pathway for the diffusion of a gap junction tracer through the incisures of Schmidt–Lanterman in *cx32*-null mice. Because of their dominant negative activity, it had been assumed that CMTX-linked Cx32 mutants co-oligomerize with wild-type connexins to form mixed connexons. We show here, however, that the R142W and E186K Cx32 mutants are not capable of assembling into connexons when expressed individually in PC12 cells, raising the possibility that they act instead by engaging wild-type connexins in some other type of complex formation or by outcompeting the normal protein for binding to an as yet unknown limiting factor required for gap junction assembly or trafficking. The gain-of-function activity of the R142W and E186K Cx32 mutants is therefore distinct from that of dominant nephrogenic diabetes insipidus-causing mutations of aquaporin-2, which is closely correlated with their ability to assemble into homo-oligomers in the absence of the wild-type protein (Kamsteeg *et al.*, 1999). Investigation of the mechanism and potential physiological significance of the dominant negative activity of R142W Cx32 and other CMTX-linked mutants awaits the definitive identification of the connexin species that coexist with Cx32 in myelinating Schwann cells.

Quality Control of Connexins in the Secretory Pathway as Revealed by CMTX-linked Cx32 Mutants

The selective recognition, retention, and degradation of incorrectly folded proteins in the secretory pathway are mediated by a variety of mechanisms that have been referred to as the cell's quality control system (Hammond and Helenius, 1995). The studies presented here indicate that there are at least three quality control processes that prevent ab-

normal connexin molecules from traversing the secretory pathway. The earliest quality control checkpoint we have identified is in the ER, where all of the E208K mutant was recognized as non-native and directed to rapid, proteasome-mediated degradation. Under all conditions tested, E208K Cx32 was detectable solely within the ER even if its turnover was slowed using inhibitors of the proteasome. ER localization of this mutant therefore appears to be due to true retention rather than to rapid degradation or to retrieval from the intermediate compartment or Golgi complex. In principle, ER retention could be due to one of three alternative processes (Kim and Arvan, 1998): 1) aggregation into insoluble complexes too large to be incorporated into a budding transport vesicle; 2) acquisition of an ER retention determinant in an otherwise normally folded protein; or 3) protein misfolding and consequent recognition by, and binding to, an ER resident. Although the basis for the transport block of E208K Cx32 is not yet known, the Triton X-100 solubility of this mutant and its inability to assemble into a connexon render the first two mechanisms unlikely and suggest instead a conformational defect consistent with the third possibility.

Some of the R142W and E186K Cx32 molecules were competent to pass through the checkpoint in the ER and entered the Golgi region. Because neither mutant assembles into connexons, the criteria for ER exit, unlike those for other multisubunit proteins (Hurtley and Helenius, 1989), cannot involve either the current or future oligomerization state. Remarkably, these two point mutants were then subjected to different post-ER quality control processes that prevented unassembled connexin monomers from reaching the cell surface. R142W Cx32 that exited the ER was transported to, and degraded within, the endosome–lysosome system. In contrast, post-ER pools of E186K Cx32 could not be detected in lysosomes but instead underwent retrograde transport from the Golgi region to the ER and remained sensitive to inhibitors of proteasomal degradation. Turnover of E186K Cx32 is therefore distinct from that of a mutant form of asialoglycoprotein receptor H1 subunit described by Wahlberg *et al.* (1995), which also exits the ER and is unaffected by lysosomal inhibitors but does not appear to return to the ER even after a 3.5-h chase with cycloheximide. Given its role in the degradation of other proteins at the ER, it is possible that the translocon mediates the dislocation of mutant connexins from the membrane into the proteasome (Plemper and Wolf, 1999). Such a process would require E186K Cx32 molecules to post-translationally reengage this channel after their return from post-ER compartments.

Degradation at the ER is also a property of wild-type connexins. As determined by pulse–chase analysis, newly synthesized WT Cx32 and Cx43 molecules continue to undergo rapid, proteasome inhibitor-sensitive turnover even if their exit from the ER is blocked with BFA (Figure 6). In this respect connexins resemble the CFTR, up to ~80% of which is destroyed by proteasome-mediated degradation in a pre-Golgi compartment (Jensen *et al.*, 1995; Ward *et al.*, 1995). Conformational maturation of the CFTR appears to be a slow and inefficient event involving interactions between domains in spatially distant regions of this polytopic membrane protein. Errors in this process are believed to result in a large population of incompletely folded CFTR molecules that are recognized by the ER degradation machinery

(Zhang *et al.*, 1998). Cysteine scanning mutagenesis has indicated that the tertiary structure of connexins may also be unusually complex, with multiple transmembrane domains contributing to the channel pore (Oh *et al.*, 1997; Zhou *et al.*, 1997). One possibility is that folding of wild-type connexins is slow relative to the rate of connexin degradation, resulting in the turnover of a large fraction of newly synthesized connexin molecules before they can achieve a conformation permissive for transport to the cell surface. Although such inefficiency would seem counterproductive, it would serve to limit the number of properly folded and therefore potentially assembly competent connexin molecules in the early secretory pathway under physiological levels of connexin expression. This would reduce the possibility of premature formation of gap junctional plaques within intracellular membranes, as has been observed after high-level overexpression of exogenous Cx32 in baby hamster kidney transfectants (Kumar *et al.*, 1995).

A common assay for assessing connexin function is the formation of intercellular channels between paired *Xenopus* oocytes injected with connexin-encoding cRNA. Bruzzone *et al.* (1994) have studied both the E186K and the R142W CMTX-linked Cx32 mutants in this system and found, as we have in PC12 cells, that these mutants are inactive. Surprisingly, both mutants appeared to accumulate at oocyte interfaces in a manner immunohistochemically indistinguishable from functional WT Cx32 and thus very different from the intracellular localization pattern observed in PC12 transfectants or (in the case of R142W Cx32) transgenic mice (Scherer *et al.*, 1999). The basis for the apparent mislocalization of the E186K and R142W Cx32 mutants in *Xenopus* oocytes is unknown. Unlike the ΔF508 mutant of the CFTR (Denning *et al.*, 1992), the trafficking defects of the CMTX-linked Cx32 mutants examined cannot be corrected by incubating PC12 cells at the lower temperatures (≤27°C) at which oocytes are maintained (our unpublished results). The slower rate of connexin degradation in oocytes relative to mammalian cells (Zhou *et al.*, 1999) is also unlikely to be a factor, in that decreasing the rate of mutant Cx32 turnover in PC12 cells with proteasome inhibitors did not induce cell surface localization. Transport to the plasma membrane after exogenous expression in oocytes, but not in mammalian cells, has also been described for some mutants of the aquaporin-2 water channel (Tamarappoo and Verkman, 1998; Yang *et al.*, 1999). Although it is conceivable that oocytes are more permissive than mammalian cells in allowing misfolded proteins to traverse the secretory pathway, it is difficult to imagine how they would avoid the toxic consequences of inappropriate localization of nonfunctional or malfunctioning proteins. A more likely explanation for the cell surface expression of the E186K and R142W Cx32 mutants observed by Bruzzone *et al.* (1994) is that oocytes have a normal quality control system but that the capacity of this system is exceeded by the very high expression levels routinely achieved after injection of cRNA into these enormous cells. Leakage of mutant or otherwise improperly folded membrane proteins to the cell surface after supraphysiological overexpression has previously been described even in mammalian cells (Maimone and Merlie, 1993; Cheng *et al.*, 1995). An alternative possibility arises from a study by Mulders *et al.* (1998) in which an aquaporin-2 mutant that by immunofluorescence microscopy appeared to be efficiently transported to the cell surface

when expressed in *Xenopus* oocytes was shown by electron microscopy to instead be localized to Golgi stacks concentrated immediately beneath the oolemma. Lack of resolution between the oolemma and Golgi is, however, unlikely to account for the observations of Bruzzone *et al.* (1994), because intracellular retention would not be expected to lead to the reported concentration of the E186K and R142W Cx32 mutants at regions of cell–cell contact.

Relevance to Other Connexin-related Disorders

Following the identification of Cx32 mutations in CMTX patients, additional human diseases have been genetically linked to members of the connexin family (Kelsell *et al.*, 1997; Richard *et al.*, 1998; Shiels *et al.*, 1998; Xia *et al.*, 1998; Mackay *et al.*, 1999). In light of our current studies, it is particularly intriguing that an R to W substitution in position 143 of Cx26, which corresponds to R142 in Cx32, is associated with nonsyndromic deafness (Brobby *et al.*, 1998) and that an E183K mutation in Cx31 (equivalent to E186K in Cx32) is found in individuals with autosomal dominant hearing impairment (Xia *et al.*, 1998). It is therefore anticipated that some of the findings reported here will be applicable to disease-causing mutations in other connexins.

REFERENCES

Anzini, P., Neuberg, D.H., Schachner, M., Nelles, E., Willecke, K., Zielasek, J., Toyka, K.V., Suter, U., and Martini, R. (1997). Structural abnormalities and deficient maintenance of peripheral nerve myelin in mice lacking the gap junction protein connexin 32. J. Neurosci. *17*, 4545–4551.

Aridor, M., and Balch, W.E. (1999). Integration of endoplasmic reticulum signaling in health and disease. Nat. Med. *5*, 745–751.

Balice-Gordon, R.J., Bone, L.J., and Scherer, S.S. (1998). Functional gap junctions in the schwann cell myelin sheath. J. Cell Biol. *142*, 1095–1104.

Beardslee, M.A., Laing, J.G., Beyer, E.C., and Saffitz, J.E. (1998). Rapid turnover of connexin43 in the adult rat heart. Circ. Res. *83*, 629–635.

Bergoffen, J., Scherer, S.S., Wang, S., Scott, M.O., Bone, L.J., Paul, D.L., Chen, K., Lensch, M.W., Chance, P.F., and Fischbeck, K.H. (1993). Connexin mutations in X-linked Charcot-Marie-Tooth disease. Science *262*, 2039–2042.

Bone, L.J., Deschenes, S.M., Balice-Gordon, R.J., Fischbeck, K.H., and Scherer, S.S. (1997). Connexin32 and X-linked Charcot-Marie-Tooth disease. Neurobiol. Dis. *4*, 221–230.

Bonifacino, J.S., and Weissman, A.M. (1998). Ubiquitin and the control of protein fate in the secretory and endocytic pathways. Annu. Rev. Cell Dev. Biol. *14*, 19–57.

Brobby, G.W., Muller-Myhsok, B., and Horstmann, R.D. (1998). Connexin 26 R143W mutation associated with recessive nonsyndromic sensorineural deafness in Africa (letter). N. Engl. J. Med. *338*, 548–550.

Brodsky, J.L., and McCracken, A.A. (1997). ER-associated and proteasome-mediated protein degradation: how two topologically restricted events came together. Trends Cell Biol. *7*, 151–156.

Bruzzone, R., White, T.W., Scherer, S.S., Fischbeck, K.H., and Paul, D.L. (1994). Null mutations of connexin32 in patients with X-linked Charcot-Marie-Tooth disease. Neuron *13*, 1253–1260.

Carlson, J.A., Rogers, B.B., Sifers, R.N., Finegold, M.J., Clift, S.M., DeMayo, F.J., Bullock, D.W., and Woo, S.L. (1989). Accumulation of PiZ alpha 1-antitrypsin causes liver damage in transgenic mice. J. Clin. Invest. *83*, 1183–1190.

Cascio, M., Kumar, N.M., Safarik, R., and Gilula, N.B. (1995). Physical characterization of gap junction membrane connexons (hemichannels) isolated from rat liver. J. Biol. Chem. *270*, 18643–18648.

Castro, C., Gomez-Hernandez, J.M., Silander, K., and Barrio, L.C. (1999). Altered formation of hemichannels and gap junction channels caused by C-terminal connexin-32 mutations. J. Neurosci. *19*, 3752–3760.

Cheng, S.H., Fang, S.L., Zabner, J., Marshall, J., Piraino, S., Schiavi, S.C., Jefferson, D.M., Welsh, M.J., and Smith, A.E. (1995). Functional activation of the cystic fibrosis trafficking mutant delta F508-CFTR by overexpression. Am. J. Physiol. *268*, L615–L624.

Cole, N.B., Sciaky, N., Marotta, A., Song, J., and Lippincott-Schwartz, J. (1996). Golgi dispersal during microtubule disruption: regeneration of Golgi stacks at peripheral endoplasmic reticulum exit sites. Mol. Biol. Cell *7*, 631–650.

Denning, G.M., Anderson, M.P., Amara, J.F., Marshall, J., Smith, A.E., and Welsh, M.J. (1992). Processing of mutant cystic fibrosis transmembrane conductance regulator is temperature-sensitive. Nature *358*, 761–764.

Deschenes, S.M., Walcott, J.L., Wexler, T.L., Scherer, S.S., and Fischbeck, K.H. (1997). Altered trafficking of mutant connexin32. J. Neurosci. *17*, 9077–9084.

D'Urso, D., Prior, R., Greiner-Petter, R., Gabreels-Festen, A.A., and Muller, H.W. (1998). Overloaded endoplasmic reticulum-Golgi compartments, a possible pathomechanism of peripheral neuropathies caused by mutations of the peripheral myelin protein PMP22. J. Neurosci. *18*, 731–740.

Fallon, R.F., and Goodenough, D.A. (1981). Five-hour half-life of mouse liver gap-junction protein. J. Cell Biol. *90*, 521–526.

Goodenough, D.A., Goliger, J.A., and Paul, D.L. (1996). Connexins, connexons, and intercellular communication. Annu. Rev. Biochem. *65*, 475–502.

Goodenough, D.A., Paul, D.L., and Jesaitis, L. (1988). Topological distribution of two connexin32 antigenic sites in intact and split rodent hepatocyte gap junctions. J. Cell Biol. *107*, 1817–1824.

Gow, A., and Lazzarini, R.A. (1996). A cellular mechanism governing the severity of Pelizaeus-Merzbacher disease. Nat. Genet. *13*, 422–428.

Gow, A., Southwood, C.M., and Lazzarini, R.A. (1998). Disrupted proteolipid protein trafficking results in oligodendrocyte apoptosis in an animal model of Pelizaeus-Merzbacher disease. J. Cell Biol. *140*, 925–934.

Graham, K.S., Le, A., and Sifers, R.N. (1990). Accumulation of the insoluble PiZ variant of human alpha 1-antitrypsin within the hepatic endoplasmic reticulum does not elevate the steady-state level of grp78/BiP. J. Biol. Chem. *265*, 20463–20468.

Greenfield, J.P., Tsai, J., Gouras, G.K., Hai, B., Thinakaran, G., Checler, F., Sisodia, S.S., Greengard, P., and Xu, H. (1999). Endoplasmic reticulum and trans-Golgi network generate distinct populations of Alzheimer beta-amyloid peptides. Proc. Natl. Acad. Sci. USA *96*, 742–747.

Hammond, C., and Helenius, A. (1995). Quality control in the secretory pathway. Curr. Opin. Cell Biol. *7*, 523–529.

Hertzberg, E.L. (1984). A detergent-independent procedure for the isolation of gap junctions from rat liver. J. Biol. Chem. *259*, 9936–9943.

Hsu, V.W., Yuan, L.C., Nuchtern, J.G., Lippincott-Schwartz, J., Hammerling, G.J., and Klausner, R.D. (1991). A recycling pathway between the endoplasmic reticulum and the Golgi apparatus for retention of unassembled MHC class I molecules. Nature *352*, 441–444.

Hurtley, S.M., and Helenius, A. (1989). Protein oligomerization in the endoplasmic reticulum. Annu. Rev. Cell Biol. *5*, 277–307.

Ionasescu, V., Ionasescu, R., and Searby, C. (1996). Correlation between connexin 32 gene mutations and clinical phenotype in X-linked dominant Charcot-Marie-Tooth neuropathy. Am. J. Med. Genet. *63*, 486–491.

Jackson, M.R., Nilsson, T., and Peterson, P.A. (1993). Retrieval of transmembrane proteins to the endoplasmic reticulum. J. Cell Biol. *121*, 317–333.

Jensen, T.J., Loo, M.A., Pind, S., Williams, D.B., Goldberg, A.L., and Riordan, J.R. (1995). Multiple proteolytic systems, including the proteasome, contribute to CFTR processing. Cell *83*, 129–135.

Kamsteeg, E.J., Wormhoudt, T.A., Rijss, J.P., van Os, C.H., and Deen, P.M. (1999). An impaired routing of wild-type aquaporin-2 after tetramerization with an aquaporin-2 mutant explains dominant nephrogenic diabetes insipidus. EMBO J. *18*, 2394–2400.

Kelsell, D.P., Dunlop, J., Stevens, H.P., Lench, N.J., Liang, J.N., Parry, G., Mueller, R.F., and Leigh, I.M. (1997). Connexin 26 mutations in hereditary non-syndromic sensorineural deafness Nature *387*, 80–83.

Kim, P.S., and Arvan, P. (1998). Endocrinopathies in the family of endoplasmic reticulum (ER) storage diseases: disorders of protein trafficking and the role of ER molecular chaperones. Endocr. Rev. *19*, 173–202.

Klausner, R.D., Donaldson, J.G., and Lippincott-Schwartz, J. (1992). Brefeldin A: insights into the control of membrane traffic and organelle structure. J. Cell Biol. *116*, 1071–1080.

Kumar, N.M., Friend, D.S., and Gilula, N.B. (1995). Synthesis and assembly of human beta 1 gap junctions in BHK cells by DNA transfection with the human beta 1 cDNA. J. Cell Sci. *108*, 3725–3734.

Laing, J.G., and Beyer, E.C. (1995). The gap junction protein connexin43 is degraded via the ubiquitin proteasome pathway. J. Biol. Chem. *270*, 26399–26403.

Laing, J.G., Tadros, P.N., Westphale, E.M., and Beyer, E.C. (1997). Degradation of connexin43 gap junctions involves both the proteasome and the lysosome. Exp. Cell Res. *236*, 482–492.

Larsen, W.J., and Tung, H.N. (1978). Origin and fate of cytoplasmic gap junction vesicles in rabbit granulosa cells. Tissue Cell *10*, 585–598.

Le, A.C., and Musil, L.S. (1998). Normal differentiation of cultured lens cells after inhibition of gap junction-mediated intercellular communication. Dev. Biol. *204*, 80–96.

Lee, D.H., and Goldberg, A.L. (1998). Proteasome inhibitors: valuable new tools for cell biologists. Trends Cell Biol. *8*, 397–403.

Mackay, D., Ionides, A., Kibar, Z., Rouleau, G., Berry, V., Moore, A., Shiels, A., and Bhattacharya, S. (1999). Connexin46 mutations in

autosomal dominant congenital cataract. Am. J. Hum. Genet. *64*, 1357–1364.

Maimone, M.M., and Merlie, J.P. (1993). Interaction of the 43 kd postsynaptic protein with all subunits of the muscle nicotinic acetylcholine receptor. Neuron *11*, 53–66.

Matlin, K.S., and Simons, K. (1983). Reduced temperature prevents transfer of a membrane glycoprotein to the cell surface but does not prevent terminal glycosylation. Cell *34*, 233–243.

Mayerhofer, A., Amador, A.G., Beamer, W.G., and Bartke, A. (1988). Ultrastructural aspects of the goiter in cog/cog mice. J. Hered. *79*, 200–203.

Mege, R.M., Matsuzaki, F., Gallin, W.J., Goldberg, J.I., Cunningham, B.A., and Edelman, G.M. (1988). Construction of epithelioid sheets by transfection of mouse sarcoma cells with cDNAs for chicken cell adhesion molecules. Proc. Natl. Acad. Sci. USA *85*, 7274–7278.

Mellman, I., Fuchs, R., and Helenius, A. (1986). Acidification of the endocytic and exocytic pathways. Annu. Rev. Biochem. *55*, 663–700.

Mulders, S.M., *et al*. (1998). An aquaporin-2 water channel mutant which causes autosomal dominant nephrogenic diabetes insipidus is retained in the Golgi complex. J. Clin Invest. *102*, 57–66.

Murakami, T., Garcia, C.A., Reiter, L.T., and Lupski, J.R. (1996). Charcot-Marie-Tooth disease and related inherited neuropathies. Medicine *75*, 233–250.

Musil, L.S. (1994). Structure and assembly of gap junctions. In: Molecular Mechanisms of Epithelial Cell Junctions: From Development to Disease, ed. S. Citi, Austin, TX: R.G. Landes, 173–194.

Musil, L.S., Cunningham, B.A., Edelman, G.M., and Goodenough, D.A. (1990). Differential phosphorylation of the gap junction protein connexin43 in junctional communication-competent and -deficient cell lines. J. Cell Biol. *111*, 2077–2088.

Musil, L.S., and Goodenough, D.A. (1991). Biochemical analysis of connexin43 intracellular transport, phosphorylation, and assembly into gap junctional plaques. J. Cell Biol. *115*, 1357–1374.

Musil, L.S., and Goodenough, D.A. (1993). Multisubunit assembly of an integral plasma membrane channel protein, gap junction connexin43, occurs after exit from the ER. Cell *74*, 1065–1077.

Oh, S., Ri, Y., Bennett, M.V., Trexler, E.B., Verselis, V.K., and Bargiello, T.A. (1997). Changes in permeability caused by connexin 32 mutations underlie X-linked Charcot-Marie-Tooth disease. Neuron *19*, 927–938.

Omori, Y., Mesnil, M., and Yamasaki, H. (1996). Connexin 32 mutations from X-linked Charcot-Marie-Tooth disease patients: functional defects and dominant negative effects. Mol. Biol. Cell *7*, 907–916.

Plemper, R.K., and Wolf, D.H. (1999). Retrograde protein translocation: ERADication of secretory proteins in health and disease. Trends Biochem. Sci. *24*, 266–270.

Ren, P., de Feijter, A.W., Paul, D.L., and Ruch, R.J. (1994). Enhancement of liver cell gap junction protein expression by glucocorticoids. Carcinogenesis *15*, 1807–1813.

Richard, G., Smith, L.E., Bailey, R.A., Itin, P., Hohl, D., Epstein, E.H., Jr., DiGiovanna, J.J., Compton, J.G., and Bale, S.J. (1998). Mutations in the human connexin gene GJB3 cause erythrokeratodermia variabilis. Nat. Genet. *20*, 366–369.

Rock, K.L., Gramm, C., Rothstein, L., Clark, K., Stein, R., Dick, L., Hwang, D., and Goldberg, A.L. (1994). Inhibitors of the proteasome block the degradation of most cell proteins and the generation of peptides presented on MHC class I molecules. Cell *78*, 761–771.

Sadeghi, H.M., Innamorati, G., and Birnbaumer, M. (1997). An X-linked NDI mutation reveals a requirement for cell surface V2R expression. Mol. Endocrinol. *11*, 706–713.

Scherer, S.S., Bone, L.J., Deschenes, S.M., Abel, A., Balice-Gordon, R.J., and Fischbeck, K.H. (1999). The role of the gap junction protein connexin32 in the pathogenesis of X-linked Charcot-Marie-Tooth disease. Novartis Found. Symp. *219*, 175–185.

Scherer, S.S., Deschenes, S.M., Xu, Y.T., Grinspan, J.B., Fischbeck, K.H., and Paul, D.L. (1995). Connexin32 is a myelin-related protein in the PNS and CNS. J. Neurosci. *15*, 8281–8294.

Scherer, S.S., Xu, Y.T., Nelles, E., Fischbeck, K., Willecke, K., and Bone, L.J. (1998). Connexin32-null mice develop demyelinating peripheral neuropathy. Glia *24*, 8–20.

Seglen, P.O. (1983). Inhibitors of lysosomal function. Methods Enzymol. *96*, 737–764.

Shiels, A., Mackay, D., Ionides, A., Berry, V., Moore, A., and Bhattacharya, S. (1998). A missense mutation in the human connexin50 gene (GJA8) underlies autosomal dominant "zonular pulverulent" cataract, on chromosome 1q. Am. J. Hum. Genet. *62*, 526–532.

Skovronsky, D.M., Doms, R.W., and Lee, V.M. (1998). Detection of a novel intraneuronal pool of insoluble amyloid beta protein that accumulates with time in culture. J. Cell Biol. *141*, 1031–1039.

Stevens, T.H., and Forgac, M. (1997). Structure, function and regulation of the vacuolar (H+)-ATPase. Annu. Rev. Cell Dev. Biol. *13*, 779–808.

Tamarappoo, B.K., and Verkman, A.S. (1998). Defective aquaporin-2 trafficking in nephrogenic diabetes insipidus and correction by chemical chaperones. J. Clin. Invest. *101*, 2257–2267.

VanSlyke, J.K., and Musil, L.S. (2000). Analysis of connexin intracellular transport and assembly. Methods *20*, 156–164.

Wahlberg, J.M., Geffen, I., Reymond, F., Simmen, T., and Spiess, M. (1995). trans-Golgi retention of a plasma membrane protein: mutations in the cytoplasmic domain of the asialoglycoprotein receptor subunit H1 result in trans-Golgi retention. J. Cell Biol. *130*, 285–297.

Ward, C.L., Omura, S., and Kopito, R.R. (1995). Degradation of CFTR by the ubiquitin-proteasome pathway. Cell *83*, 121–127.

Xia, J.H., *et al*. (1998). Mutations in the gene encoding gap junction protein beta-3 associated with autosomal dominant hearing impairment. Nat. Genet. *20*, 370–373.

Yang, B., Ma, T., Xu, Z., and Verkman, A.S. (1999). cDNA and genomic cloning of mouse aquaporin-2: functional analysis of an orthologous mutant causing nephrogenic diabetes insipidus. Genomics *57*, 79–83.

Yoshimura, T., Satake, M., Ohnishi, A., Tsutsumi, Y., and Fujikura, Y. (1998). Mutations of connexin32 in Charcot-Marie-Tooth disease type X interfere with cell-to-cell communication but not cell proliferation and myelin-specific gene expression. J. Neurosci. Res. *51*, 154–161.

Zhang, F., Kartner, N., and Lukacs, G.L. (1998). Limited proteolysis as a probe for arrested conformational maturation of delta F508 CFTR. Nat. Struct. Biol. *5*, 180–183.

Zhou, L., Kasperek, E.M., and Nicholson, B.J. (1999). Dissection of the molecular basis of pp60(v-src) induced gating of connexin 43 gap junction channels. J. Cell Biol. *144*, 1033–1045.

Zhou, X.W., Pfahnl, A., Werner, R., Hudder, A., Llanes, A., Luebke, A., and Dahl, G. (1997). Identification of a pore lining segment in gap junction hemichannels. Biophys. J. *72*, 1946–1953.